Pramana – J. Phys. (2022) 96:224
https://doi.org/10.1007/s12043-022-02473-1

Gravastars with cylindrical space–time in $f(G, T)$ gravity

M Z BHATTI*, Z YOUSAF and A REHMAN

Department of Mathematics, University of the Punjab, Quaid-i-Azam Campus, Lahore 54590, Pakistan
*Corresponding author. E-mail: mzaeem.math@pu.edu.pk, zeeshan.math@pu.edu.pk, attiqwatto786@gmail.com

MS received 13 January 2022; revised 29 April 2022; accepted 4 August 2022

Abstract. The aim of this paper is to investigate the formation and evolution of the celestial object, known as gravastar. The idea of this gravitationally vacuum star is suggested by Mazur and Mottola. In general, the gravastar is assumed to be composed of three distinct regions. These regions are explained thoroughly with the help of certain equations of states and the values of metric coefficients corresponding to these sectors are also determined. The perfect fluid and cylindrically symmetric metric are assumed to derive Bianchi identities and modified field equations. The internal and external geometries are combined with each other at intermediate thin shell and specific conditions are used for this purpose. In the framework of an alternative gravitational theory, i.e., $f(G, T)$ theory, we calculate a regular solution for gravastar along with the elaboration of specific substantial attributes of the model. The significance of $f(G, T)$ theory for attaining gravastar model is also studied.

Keywords. Cosmology; general relativity; spatial singularity; density.

PACS Nos **04.70.Bw; 04.70.Dy; 11.25.-w**

1. Introduction

The study about the eventual demise of a compact star has significant importance in cosmology and astrophysics. According to virial theorem, a star will be able to retain its stability if its gravitational potential energy is twice its internal thermal energy. It is a challenging task for a compact star to balance the force of attraction exerted by the internal gravity after consuming all its fuel. As a result, new celestial objects are devised, and this event is known as gravitational collapse. Neutron stars, white dwarfs and black holes (BHs) are among the celestial objects devised as a consequence of gravitational collapse. The BH has been the most interesting compact object in cosmology in the context of GR, and its formation depends upon the mass of the collapsing star. Because of the tremendous density and compact structure of BH, it is impossible for anything to escape out of it. In our galaxy, the presence of hundreds of stellar-mass BHs, i.e., 10^8 is predicted. The existence of a supermassive BH having mass from 10^6 to 10^9 times the mass of a Sun is assumed at the centre of each galaxy. Therefore, many BHs are probably present in our Universe.

If we analyse the gravitational effects at quantum level, then it might be conceivable that no event horizon is formed at the end of gravitational collapse and in this particular case, no BH is formed. Following this consideration, formation of many celestial objects without event horizon have been proposed as alternative to BH. Mazur and Mottola (MM) [1] suggested a gravitationally vacuum compact object known as gravastar as a feasible alternative to BH. For this purpose, they broadened the conception of Bose–Einstein condensation (BEC) to the gravitating system. In the BEC state, due to the continuous decrease in the temperature of gas molecules, their velocities become insignificant. Afterwards, so many researchers have analysed this gravastar model under different perspectives [2,4–6]. Gravastar is generally hypothesised to be comprised of three sectors. The interior sector of the gravastar is under the influence of a substance whose negative pressure must be equal to its energy density.

Due to the dominance of negative pressure in the interior sector, it exerts repulsive force which consequently ceases the creation of singularity in it. There is a thin shell at the end of the internal sector, which is considered to comprise ultrarelativistic substance. This stiff fluid was originally proposed by Zel'dovich [7] to explain matter with high pressure. The speed of sound and speed of light is claimed to be equal for these types of matter. The shell thickness is considered to be very little having range $r_1 < r < r_2$ where r_1 is the radius of the interior sector and $r_2 = r + \epsilon$ is the radius of the exterior

Published online: 25 November 2022

sector (ϵ indicates the thickness of shell). The exterior of the gravastar is totally a vacuum and we explain it with the help of Schwarzschild, Reissner Nordström or Kerr–Newmann metrics depending upon the considered conditions of our model. We use different equations of states to interpret distinct sectors of gravastar. In the literature, a great deal of work related to the mathematical and theoretical analyses of gravastar is available [8–15]. They considered the complete conversion of gravitating mass of the interior sector into the electromagnetic mass because of the existence of electric charge in it.

Banerjee *et al* [16] analysed the brane-world gravastar formation in the context of alternative theory of gravity. They also calculated the regular solutions related to distinct regions of the gravastar. The dipolar magnetic field formation along with the solution of Maxwell field equations was studied by Turimov *et al* [17]. Kubo and Sakai [18] investigated distinct methods for the detection of gravastars through their gravitational results. Horvat *et al* [19] investigated the influence of electric charge on gravastar model. They considered the coupling between electric field and fluid energy density to solve the Einstein–Maxwell field equations. Ghosh *et al* [20] calculated a regular solution for higher-dimensional gravastar models by consolidating the Karmarkar condition. They derived an exact solution corresponding to intermediate thin shell without considering the relevant approximation. Yousaf *et al* [21,22] investigated the influence of electromagnetic field on the structural configuration of string-like axially symmetric objects by using the framework of an alternative gravity theory. Bhatti *et al* [23–26] considered cylindrically symmetric space–time and thin shell formulation for elaborating distinct regions of gravastar and also studied the stability of compact objects.

The beginning, growth and present situation of gravastar have been analysed by Ray *et al* [27]. They also analysed different gravastar models by using the mathematical formulation of distinct alternative theories. The presence of large stable areas in static gravastar model makes it a difficult task to distinguish it from a classical BH. However, Harko *et al* [28] concluded that rotating gravastars can be differentiated from Kerr-type black holes by the thorough study of accretion disks around them. Ghosh *et al* [29] evaluated higher-dimensional gravastar model along with the cosmological constant Λ. After considering the three-layered model of gravastar, they derived singularity-free and stable solutions for the model. Bhatti *et al* [30] discussed the physical attributes of the gravastars in the background of an alternative gravity. They also analysed the impact of $f(R, G)$ theory on the stability of gravastars.

In the case of gravastars, at the time of development of the event horizon, a quantum phase transition is supposed to take place due to which the formation of event horizon is avoided. Due to the existence of large stable areas at the predicted position of the event horizon, it is a difficult task to distinguish a gravastar from a BH. Dilemma of singularity and event horizon have been the points of concern for scientists since the discovery of BH. Gravastar is considered as one of the most interesting compact object for the analysis in these days, because it resolves the problem of singularity and event horizon. Event horizon is a boundary which is hypothesised around the compact object after which all physics laws break down. In the beginning of the Universe and at the end of gravitational collapse, tremendous amount of energy was concentrated at a small area. GR predicts the formation of singularity in these situations [31]. Although GR is acknowledged as an efficient theory for describing many cosmological and astrophysical events, it somehow cannot describe BH in a proper way. The theory was questioned by observatory findings on the absence of event horizon.

At the early stages, most scientists thought that our Universe is static. In their stationary model of Universe, Gold and Bondi suggested that Universe should not be concerted at any point and time had no particular origin. Afterwards, they claimed that constant density of the Universe is resulted by continuous formation of matter. The idea of the expanding Universe is more realistic than the static one. The expanding Universe was firstly claimed by Wirtz. After observing red-shift light from galaxies, Slipher claimed that the distance of galaxies from us is continuously increasing. Latest findings from some observatory evidences, such as type-Ia supernova, cosmic microwave background radiations, etc., [32] predicted the extension of Universe at accelerated rate. Alternative gravity theories provide more efficient framework for describing the expansion of our Universe. These theories are developed after a suitable change in the Einstein–Hilbert action. Nojiri and Odintsov [33] elaborated both the significance and use of these alternative theories in detail. The addition of Gauss–Bonnet invariant G in Einstein–Hilbert action results in $f(G)$ theory of gravity.

Easson [34] analysed the delayed cosmic acceleration with the help of the formulation of $f(G)$ theory. The Gauss–Bonnet dark energy model was proposed by Nojiri *et al* [35] after being inspired by the string theory. They further revealed that the current expansion of our Universe can be the combined effect of scalar phantom and string impacts. Neupane and Carter [36] suggested a cosmological model by considering the coupling between the Gauss–Bonnet invariant and the effective action. Sharif and Ikram proposed $f(G, T)$ gravity theory and derived distant energy restrictions related to FRW metric. They deduced that the important

test particles will follow non-geodesic path due to the existence of dynamical forces. We can define delayed cosmic acceleration in different ways by considering certain models corresponding to $f(G,T)$ gravity theory. Bhatti *et al* [37,38] analysed the development of distinct celestial stars in the context of $f(G,T)$ gravity. The impact of alternative theory on sustainability of the compact star was also elaborated by using graphs. The explicit framework of the manuscript is as follows: The fundamental formalism of $f(G,T)$ is given in §2. The field equations along with the non-conservation equation related to $f(G,T)$ theory are also derived in this section. Section 3 is committed for the analysis of the construction of gravastar in addition to the mathematical evaluation of distinct sectors of our model. Junction conditions are explored in §3 to enable even coupling between the interior de-Sitter space–time and the exterior Schwarzschild space–time. Section 5 deals with the study of physical attributes of the gravastars and their dependence on the thickness of the shell is demonstrated graphically. Significant outcomes of our paper are stated in §6.

2. $f(G,T)$ Gravity and field equations

In this section, we shall analyse the basic formulism of $f(G,T)$ theory of gravity along with the solution of the corresponding field equations. We initiate with modified Einstein–Hilbert action for $f(G,T)$ gravity which is written as [39]

$$S = \frac{1}{2\kappa^2}\int \sqrt{-g}R\mathrm{d}^4x + \frac{1}{2\kappa^2}\int \sqrt{-g}f(G,T)\mathrm{d}^4x + \int L_m\sqrt{-g}\mathrm{d}^4x, \tag{1}$$

where the function $f(G,T)$ combines the Gauss–Bonnet invariant G with the trace of energy momentum tensor T and g indicates the metric determinant. Furthermore, κ is the coupling constant, R is the Ricci scalar and L_m is the matter Lagrangian. The variation of eq. (1) corresponding to the metric tensor $g_{\alpha\beta}$, gives the field equations as

$$\begin{aligned} G_{\alpha\beta} &= T_{\alpha\beta} + 2Rg_{\alpha\beta}\nabla^2 f_G \\ &\quad +2R\nabla_\alpha\nabla_\beta f_G + 4g_{\alpha\beta}R^{\zeta\eta}\nabla\zeta\nabla\eta f_G \\ &\quad +4R_{\alpha\beta}\nabla^2 f_G - 4R^\zeta_\alpha\nabla_\beta\nabla_\zeta f_G \\ &\quad -4R^\zeta_\beta\nabla_\alpha\nabla_\zeta f_G - 4R_{\alpha\zeta\beta\eta}\nabla^\zeta\nabla^\eta f_G \\ &\quad \times\frac{1}{2}g_{\alpha\beta}f - T_{\alpha\beta}f_T + 2T_{\alpha\beta}f_T + pg_{\alpha\beta}f_T \\ &\quad -2RR_{\alpha\beta}f_G + 4R^\zeta_\alpha R_{\zeta\beta}f_G \\ &\quad +4R_{\alpha\zeta\beta\eta}R^{\zeta\eta}f_G - 2R^{\zeta\eta\delta}_\alpha R_{\beta\zeta\eta\delta}f_G. \end{aligned} \tag{2}$$

Here, de-Alembertian operator is represented by $\nabla^2 = \nabla^\alpha\nabla_\alpha$, $G_{\alpha\beta} = R_{\alpha\beta} - \frac{1}{2}g_{\alpha\beta}R$ is written for the Einstein tensor, whereas

$$f_G \equiv \frac{\partial f(G,T)}{\partial G}$$

and

$$f_T \equiv \frac{\partial f(G,T)}{\partial T}.$$

It is worthy to mention that the field equations corresponding to $f(G)$ can be obtained by considering $f(G)$ instead of $f(G,T)$ in eq. (2). The following cylindrically static metric will be used to derive the regular solution of our model

$$\mathrm{d}s^2 = -B(r)\mathrm{d}t^2 + C(r)\mathrm{d}r^2 + r^2\mathrm{d}\phi^2 + r^2\alpha^2\mathrm{d}z^2, \tag{3}$$

where

$$B(r) = \frac{1}{C(r)}$$

and

$$B(r) = \sqrt{\xi^2r^2 - \frac{4M}{\xi r}}$$

while ξ is a constant and M specifies the mass of the gravitational system. To describe the locally isotropic matter of our model, we shall use the following stress energy tensor:

$$T^{(\mathrm{mat})}_{\alpha\beta} = (\rho + p)u_\alpha u_\beta + pg_{\alpha\beta}. \tag{4}$$

The four velocity of matter is denoted by u and p is the fluid pressure. The distinct scale factor values corresponding to the internal region of the gravastar have significant importance in calculating the gravitating mass of the gravastar. The solution of modified field equations is necessary in this regard. The non-zero Einstein tensor components pertaining to the considered geometry are stated as

$$G_{00} = -\frac{B}{r^2C} + \frac{BC'}{rC^2}, \tag{5}$$

$$G_{11} = \frac{1}{r^2} + \frac{B'}{rC}, \tag{6}$$

$$G_{22} = G_{33} = -\frac{r^2B'C'}{4BC^2} + \frac{-rC'}{2C^2} + \frac{rB'}{2BC} + \frac{rB'}{BC} + \frac{r^2B''}{2BC} - \frac{r^2B'^2}{4B^2C} - \frac{rC'}{C^2}. \tag{7}$$

Here, prime indicates differentiation corresponding to r in the preceding equations. Using eqs (3)–(7) in (2), the modified field equations turn out to be

$$C'r - C = r^2C^2\left[\rho + \rho f_T - pf_T + \chi^0_0\right], \tag{8}$$

$$B + rB' = Cr^2 B\left[p + 2pf_T + \chi_1^1\right], \tag{9}$$

$$r^2\left[p + 2pf_T + \chi_2^2\right] = \left[\frac{r^2B''}{2BC} + \frac{rB'}{2BC} - \frac{rC'}{2C^2} + \frac{rB'}{BC} - \frac{r^2B'C'}{4BC^2} - \frac{r^2B'^2}{4B^2C}\right]. \tag{10}$$

The dark source terms are represented by χ_0^0, χ_1^1 and χ_2^2. The non-conservation equation given below will be useful for calculating the values of metric coefficients

$$\begin{aligned}&\frac{P'}{C} + \chi^{11'(D)} + \frac{\rho B'}{2BC} + \frac{B'}{2C}\chi^{00} \\ &+\frac{C'}{2C}\chi^{11} - \frac{r}{C}\chi^{22} - \frac{\alpha^2 r}{C}\chi^{33} + \frac{C'}{2C}\chi^{11} \\ &+\frac{PB'}{2BC} + \frac{B'}{2B}\chi^{11} + \frac{2}{r}\chi^{11} \\ &+2\left(\frac{P}{C}\right)f_T' + 2\left(\frac{P}{C}\right)' f_T + \frac{\rho B'}{2BC}f_T \\ &+\frac{PC'}{C^2}f_T + \frac{2P}{C}f_T + \frac{4P}{rC}f_T = S^\star.\end{aligned} \tag{11}$$

The value of $S^\star$ is given in Appendix. Now, eq. (8) along with the assumption that energy density is constant, implies the following value of C^{-1}:

$$\begin{aligned}C^{-1} =& \frac{8C}{r}\int r^2\rho f_T \mathrm{d}r + \frac{8}{r}\int r^2\chi_0^0 \mathrm{d}r \\ &-\frac{8C}{r}\int r^2 p f_T \mathrm{d}r + \frac{1}{4\pi} + 2 - \frac{16m}{\alpha r}.\end{aligned} \tag{12}$$

In eq. (12) gravitational mass is indicated by m whereas r is the radius of the inner sector of the gravastar.

3. Gravastar configuration

The different regions of cylindrically symmetric gravastar will be evaluated and relevant results will be determined in this section. The thin shell of the gravastar model is supposed to be made up of stiff fluid and inspection of this particular fluid will play a vital role in matching different space–times.

3.1 *Interior region*

According to the primary model recommended by MM, the interior sector of the gravastar cannot be a vacuum. We shall use $p = -\rho$ as EoS to explain this sector. This EoS illustrates the repelling nature of the interior sector which is generated due to the domination of dark energy in it. This repulsive force consequently prevents the development of singularity in the gravastar. The non-appearance of singularity in the gravastar is of significance to differentiate it from the black holes. The law of non-conservation defined in eq. (11) with the above specified EoS results in the following equation:

$$\rho = -\rho_0(\text{constant}) \tag{13}$$

and pressure is written as

$$p = -\rho_0. \tag{14}$$

The use of eq. (14) in (11) will give the value of C^{-1} as follows:

$$\begin{aligned}C^{-1} =& r\int \chi_0^0 \mathrm{d}r - \frac{2}{r}\int\left(\int \chi_0^0 \mathrm{d}r\right) r\mathrm{d}r \\ &-\frac{\rho_0 r^2}{3} - \rho_0 r\int f_T \mathrm{d}r \\ &-\frac{2\rho_0}{r}\int\left(\int f_T \mathrm{d}r\right) r\mathrm{d}r + \frac{1}{r}\int p r^2 f_T \mathrm{d}r + \frac{A}{r}.\end{aligned} \tag{15}$$

The viable solution is only possible in the case of $A = 0$, so that

$$\begin{aligned}C^{-1} =& r\int \chi_0^0 \mathrm{d}r - \frac{2}{r}\int\left(\int \chi_0^0 \mathrm{d}r\right) r\mathrm{d}r \\ &-\frac{\rho_0 r^2}{3} - \rho_0 r\int f_T \mathrm{d}r \\ &-\frac{2\rho_0}{r}\int\left(\int f_T \mathrm{d}r\right) r\mathrm{d}r + \frac{1}{r}\int p r^2 f_T \mathrm{d}r.\end{aligned} \tag{16}$$

The use of eqs (8), (9), (13) and (14) gives the dependency of metric potentials as follows:

$$B = ZC^{-1} + \mathrm{e}^{s(r)}. \tag{17}$$

In above equation, Z is the constant of integration and mathematical expression for $s(r)$ is given in Appendix. The expression for gravitating mass $M(D)$ is determined as

$$\begin{aligned}M(D) =& \frac{\alpha r^2}{2}\int \chi_0^0 \mathrm{d}r - \frac{\alpha}{2}\int\left(\int \chi_0^0 \mathrm{d}r\right) r\mathrm{d}r \\ &+\frac{\alpha r^3\rho_0}{2} + \frac{\alpha\rho_0 r^2}{2}\int f_T \mathrm{d}r \\ &-\alpha\rho_0\int\left(\int f_T \mathrm{d}r\right) r\mathrm{d}r \\ &-\frac{\alpha}{2}\int r^2 p f_T \mathrm{d}r + \frac{\alpha r}{8}.\end{aligned} \tag{18}$$

Equation (18) serves as a link between the gravitating mass M and radial coordinate r and is considered to be a vital attribute of our model. The integral given in

the above equation will behave as improper integral at $r = \infty$ which is not a sustainable value.

3.2 *Intermediate thin shell*

At the edge of the interior sector, the existence of intermediate thin shell is assumed which comprises ultrarelativistic matter. The construction of this thin shell will be assessed by using $p = \rho$ as EoS in this subsection. This EoS implies the equality between density and pressure of the intermediate shell and concedes that there is no vacuum in it. Consequently, we say that the shell consists of stiff fluid. The study of this fluid has particular significance in understanding many cosmological and astrophysical developments. To retain the sustainability of our model, the intermediate shell generates the gravitating force which balances the force of repulsion applied by the interior sector. The length, entropy and energy of the shell are related directly with its thickness. Furthermore, the role of the shell thickness is crucial in describing the physical characteristics of the gravastar. Since it is not easy to find the solution of field equations in the absence of pressure, we shall make necessary approximations to derive a feasible solution. The value of C will be $0 < C < 1$, due to the smaller values of metric coefficients. The use of eqs (8)–(10) along with the above assumptions results in the following equations:

$$\frac{\mathrm{d}}{\mathrm{d}r}\left(\frac{1}{C}\right) = r\chi_0^0 + r\chi_1^1 + 2prf_T. \tag{19}$$

$$\left[\frac{B'}{4B} + \frac{3}{r}\right]\frac{\mathrm{d}}{\mathrm{d}r}\left(\frac{1}{C}\right) = \chi_0^0 + \chi_2^2 + 2pf_T. \tag{20}$$

The integration of eq. (19) gives

$$\frac{1}{C} = \int r\chi_0^0 \mathrm{d}r + \int r\chi_1^1 \mathrm{d}r + 2\int prf_T \mathrm{d}r + D, \tag{21}$$

where D is the constant of integration and its value will be less than 1 because $\epsilon \ll 1$ and $C \ll 1$. After using eqs (19) and (20), we can write

$$H = \mathrm{e}^{4\int \frac{\delta_2(r)}{\delta_1(r)}\mathrm{d}r} + Mr^{-12}. \tag{22}$$

The values of $\delta_1(r)$ and $\delta_2(r)$ are written in Appendix and M is the integration constant. The use of $p = \rho$ in the non-conservation equation results in the following equation:

$$p = \rho = \int CT^{\star}(r)\mathrm{d}r + h. \tag{23}$$

Here h is the constant of integration and the expression for $T^{\star}(r)$ can be seen in Appendix. We conclude from eq. (23) that the density of the shell will be changed immediately with the variation in its radius. Consequently, we can say that the shell will be more denser at its outer edge. Furthermore, figure 1 demonstrates the direct relation between density and pressure of the stiff matter.

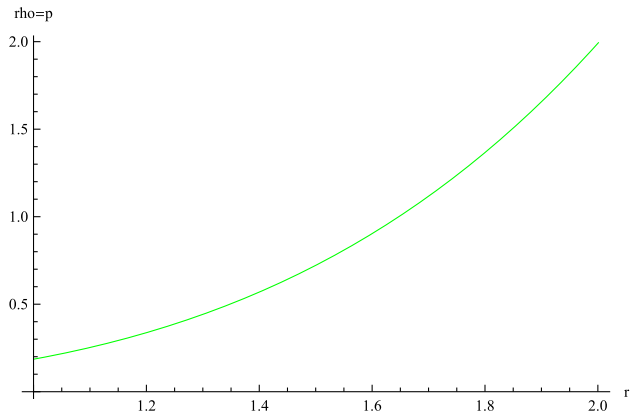

Figure 1. Graphical depiction of density (km^{-2}) vs. r (km).

3.3 *Exterior region*

The exterior of the gravastar model will be thoroughly illustrated after using $p = \rho = 0$ as the EoS. This equation means that the outside is completely a vacuum. For the characterisation of the exterior sector, we shall use the following cylindrically static metric:

$$\begin{aligned}\mathrm{d}s^2 &= -\left(1 - \frac{r^2}{\gamma^2}\right)\mathrm{d}t^2 + \left(1 - \frac{r^2}{\gamma^2}\right)^{-1}\mathrm{d}r^2 \\ &\quad + r^2\left(\mathrm{d}\phi^2 + \gamma^2\mathrm{d}z^2\right).\end{aligned} \tag{24}$$

Here γ is a constant.

4. Matching conditions

Now, we are intended to devise junction conditions to enable an even coupling between inner de-Sitter space–time and outer Schwarzschild space–time. Distinct mathematical formulations will be utilised in this regard. In our paper, we use junction conditions introduced by Darmois and Israel [40,41]. The persistence of metric coefficients at the surface $r = D$ is the mandatory condition for manipulating these conditions. These conditions have a key role in calculating the mathematical expressions for surface stress energy. The Lanczos equation and junction conditions in various gravity theories [42–45] give the expression for S_ϑ^θ as follows:

$$S_\vartheta^\theta = -\frac{1}{8\pi}\left(\kappa_\vartheta^\theta - \delta_\vartheta^\theta\kappa_k^k\right). \tag{25}$$

Here, $k_{\theta\vartheta} = K^{+}_{\theta\vartheta} - K^{-}_{\theta\vartheta}$ specifies the discontinuity corresponding to the extrinsic curvatures at the hypersurface. The $-$ sign indicates the inner region whereas $+$ indicates the exterior region. The second fundamental form [46] linked with inner and outer boundaries of the shell is written as

$$K^{\pm}_{\theta\vartheta} = -n^{\pm}_{\varrho}\left[\frac{\partial^2 x_{\varrho}}{\partial\xi^{\theta}\partial\xi^{\vartheta}} + \Gamma^{\varrho}_{\zeta\eta}\frac{\partial x^{\zeta}}{\partial\xi^{\theta}}\frac{\partial x^{\eta}}{\partial\xi^{\vartheta}}\right]_{\Sigma}, \tag{26}$$

where ξ^{ϑ} specifies the intrinsic coordinates of the shell and $n^{\pm}_{\varrho}$ indicates the unit normal to the surface so that $n^{\pm}_{\varrho}$ is written as

$$n^{\pm}_{\varrho} = \pm\left|g^{\mu\nu}\frac{\partial f}{\partial x^{\mu}}\frac{\partial f}{\partial x^{\nu}}\right|^{\frac{-1}{2}}\frac{\partial f}{\partial x^{\varrho}}, \tag{27}$$

while $n^{\alpha}n_{\alpha} = 1$. The stress energy tensor $S_{ij} = \text{diag}\,[\sigma, -\upsilon]$ is determined with the help of the Lanczos equation. The surface energy density is shown by σ whereas υ specifies the surface pressure. Equations (28) and (29) give the expressions for σ and υ, respectively, as

$$\sigma = -\frac{1}{4\pi D}\left[\sqrt{f}\right]^{+}_{-}, \tag{28}$$

$$\upsilon = -\frac{\sigma}{2} + \frac{1}{16\pi}\left[\frac{f'}{\sqrt{f}}\right]^{+}_{-}. \tag{29}$$

By considering the above two equations, we can write

$$\sigma = \frac{-1}{4\pi D}\left[\sqrt{1-\frac{D^2}{\gamma^2}} - \sqrt{\delta_0(D)}\right], \tag{30}$$

$$\upsilon = \frac{1}{8\pi D}\left[\frac{1-\frac{2D^2}{\gamma^2}}{\sqrt{1-\frac{D^2}{\gamma^2}}} - \frac{\delta_0(D) + \frac{D\delta_0'(D)}{2}}{\sqrt{\delta_0(D)}}\right]. \tag{31}$$

The value of surface energy density will be helpful in determining the total mass of the cylindrically symmetric gravastar system.

5. Important features of the gravastar

This section aims to evaluate some significant attributes of the gravastar model. Specifically, energy, entropy and length of the shell will be analysed. Furthermore, the dependence of these physical characteristics on the shell thickness will be demonstrated by plotting graphs.

5.1 *Length of the shell*

We assumed that $r_1 = D$ and $r_2 = D + \epsilon$ are the radii of the inner and outer regions of the gravastar. The thickness has been considered to be $\epsilon \ll 1$ which means that there will be small change in the length of the shell. The length of the shell is determined by using eq. (21) as

$$\ell = \int_{D}^{D+\epsilon}\sqrt{C(r)}\mathrm{d}r = \int_{D}^{D+\epsilon}\frac{\mathrm{d}r}{\sqrt{\int r\chi_0^0\mathrm{d}r + 2\int prf_T\mathrm{d}r + \int r\chi_1^1\mathrm{d}r + D}}. \tag{32}$$

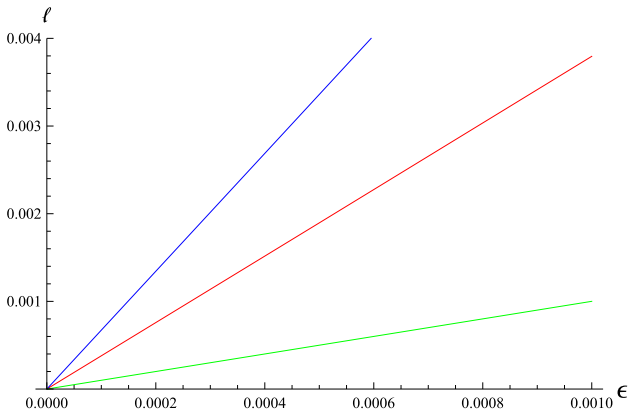

Figure 2. Graphical illustration of the relation between shell thickness ϵ (km) and proper length ℓ (km).

This equation cannot be integrated, and so we shall plot a graph to understand its physical interpretation. Figure 2 specifies the immediate change in the radial coordinate which is predicted for the construction of the gravastar. This graph also reveals the direct relationship between length and thickness of the shell.

5.1.1 *Energy content.* The EoS related to the inner sector $P = -\rho$, concedes the domination of negative pressure in it. The formation of singularity in the gravastar is averted due to the repulsive force exerted by the interior sector. The thickness of the shell has a key role in determining its energy

$$\epsilon = \int_{D}^{D+\epsilon}4\pi\rho r^2\mathrm{d}r = 4\pi\int_{D}^{D+\epsilon}\left(\int CT^{\star}(r)\mathrm{d}r + h\right)r^2\mathrm{d}r. \tag{33}$$

5.1.2 *Entropy.* The assessment of disturbance inside a celestial object is called its entropy. The size of the event horizon has certain significance in determining the entropy of BH. But, in the case of gravastar, the absence of event horizon implies the dependence of its entropy on the thickness of the shell. According to MM, entropy of the interior region must be zero, but entropy

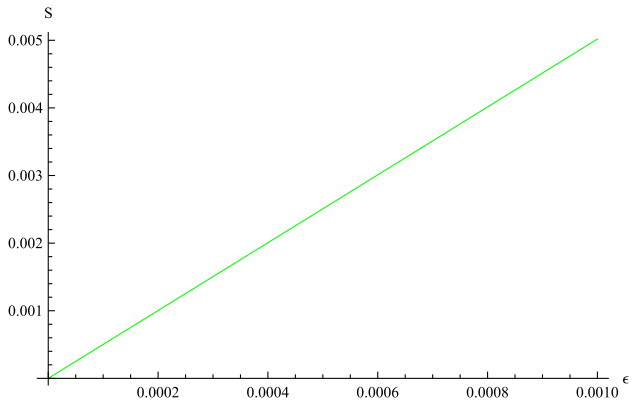

Figure 3. Graphical representation of the relation between entropy S (km) and shell thickness ϵ (km).

related with the shell is determined as

$$S = 4\pi \int_{D}^{D+\epsilon} \sqrt{C(r)} s(r) r^2 \mathrm{d}r. \tag{34}$$

The value of entropy density corresponding to the local temperature will be

$$s(r) = \frac{\psi^2 k_B^2 T(r)}{4\pi h^2} = \psi \left(\frac{k_B}{h}\right) \sqrt{\frac{p}{2\pi}}, \tag{35}$$

where ψ is a constant having no dimension and $T(r)$ represents the specific temperature. Furthermore, we assumed Planckian constant to be equal to 1. Finally, we write the expression for entropy density as follows:

$$s(r) = \psi \sqrt{\frac{p}{2\pi}} = \frac{\psi}{\sqrt{2\pi}} \sqrt{\left(\int C T^{\star}(r) \mathrm{d}r + h\right)}. \tag{36}$$

The entropy corresponding to the shell is

$$S = \frac{4\pi\alpha}{\sqrt{2\pi}} \int_{D}^{D+\epsilon} r^2 \sqrt{\left(C \int T^{\star}(r) \mathrm{d}r + h\right)} \times \frac{\mathrm{d}r}{\sqrt{\int r \chi_0^0 \mathrm{d}r + 2\int p r f_T \mathrm{d}r + \int r \chi_1^1 \mathrm{d}r + D}}. \tag{37}$$

Figure 3 reveals the direct dependence of entropy S of shell on its thickness ϵ.

5.1.3 *Equation of state.* Numerous EoSs are used to scrutinise different astrophysical phenomena [47]. The state variables that specify the states of matter within the particular physical contexts are related with each other in an EoS. It is also important to understand the distribution of different fluids and the interior evolution of celestial objects. It is not conceivable to characterise all sorts of substances by considering a single EoS. We use ideal gas law as EoS for the illustration of the dependence of gas densities on their temperature. On the other hand, perfect fluid EoS is utilised in cosmology to evaluate the interior structure of different stellar objects. Furthermore, we consider barotropic EoS for the depiction of barotropic fluids. The use of state variables is crucial in describing the physical attributes of a model. Surface pressure and surface energy density are considered to be the state variables. The EoS given below is a barotropic EoS which signifies the correspondence between these state variables as

$$\upsilon = \omega(D)\sigma. \tag{38}$$

With the help of eqs (30) and (31) in (38), we can write

$$\omega(D) = \frac{\left[\frac{1-\frac{2D^2}{\gamma^2}}{\sqrt{1-\frac{D^2}{\gamma^2}}} - \frac{\delta_0(D)+\frac{D\delta_0'(D)}{2}}{\sqrt{\delta_0(D)}}\right]}{2\left[\sqrt{\delta_0(D)} - \sqrt{1-\frac{D^2}{\gamma^2}}\right]}. \tag{39}$$

There must be positive terms in eq. (39) to derive a valid solution. We use binomial series and avoid the highly ordered terms for this purpose

$$\omega(D) \approx \frac{1}{2}\left[\frac{1 - \frac{3D^2}{2\gamma^2} - \left(\frac{2\delta_0(D)+D\delta_0(D)}{2\delta_0(D)}\right)}{\frac{D^2}{2\gamma^2} - 1 + \sqrt{\delta_0(D)}}\right]. \tag{40}$$

The distinct values of $\omega(D)$ will be helpful in analysing the interior sector and intermediate thin shell. In this way, this constraint will have substantial significance in the evaluation of gravastar formation.

6. Conclusion

Our research mainly aims to study the presence and structural configuration of a compact object known as the gravastar. The necessary formalism of an alternative theory of gravity, i.e., $f(G,T)$ is discussed. Additionally, we considered perfect fluid and cylindrically symmetric geometry for the calculation of modified field equations and non-conservation law associated with the $f(G,T)$ theory. The gravastar is a gravitationally vacuum star suggested by MM and is considered as a feasible alternative to the BH. The BH has been the most interesting compact object in cosmology and due to its highly compact nature, nothing can escape out of it. According to the primitive model, gravastar must be comprised of three sectors. We have used specific EoS corresponding to each sector for the elaboration of gravastar structure. The EoS related to the interior sector revealed the domination of negative pressure and due to the repulsive force generated by the negative pressure, singularity is not formed in the gravastar. The presence of thin shell comprised of ultrarelativistic matter is assumed at the end of the interior region. The EoS

used for the elaboration of intermediate shell claimed the equality between pressure and density for the fluid within it. The exterior of the gravastar is completely a vacuum. Distinct physical characteristics of the gravastar model have been thoroughly analysed along with the graphical demonstration of their dependence on the thickness of the intermediate thin shell. The major findings of our paper are

1. Characterisation of density and pressure: (i) In the interior sector of the gravastar, negative pressure will maintain its nature. Moreover, the values of pressure and energy density will be persistent. (ii) Figure 1 indicates the change in pressure of the ultrarelativistic fluid within the shell related to r, which is the radial coordinate. Therefore, we can assume that the outer edge of the shell will have more density than the inner one.
2. Length of the shell: We examined the relationship between the length of the intermediate shell and its thickness in the presence of effective matter. The graph (figure 2) between these two physical characteristics of the model shows the continuous increase in length with the increase in its thickness.
3. Entropy: (i) The area of the event horizon of the black hole is used to determine its entropy. Due to the absence of event horizon in the case of gravastar, its entropy will be dependent on the thickness of the shell. (ii) Figure 3 shows that by increasing (decreasing) the shell thickness (ϵ), its entropy (S) will also increase (decrease).

Appendix

The extra curvature terms appearing in our analysis are given as

$$\begin{aligned}
\chi_{00} &= \frac{B'^2C'}{BC^3}f'_G - \frac{B'C'}{C^3}f''_G + \frac{5B'C'^2}{4C^4}f'_G \\
&\quad - \frac{10B'C'}{rC^3}f'_G + \frac{B'B''}{BC^2}f'_G + \frac{2B''}{C^2}f''_G \\
&\quad - \frac{3B''C'}{2C^3}f'_G + \frac{6B''}{rC^2}f'_G - \frac{B'^3}{2B^2C^2}f'_G \\
&\quad - \frac{B'^2}{2BC^2}f''_G - \frac{2B'^2}{rBC^2}f'_G \\
&\quad + \frac{6B'}{rC^2}f''_G + \frac{19B'}{r^2C^2}f'_G - \frac{BC'}{rC^3}f''_G - \frac{9BC'}{r^2C^3}f'_G \\
&\quad + \frac{20B}{r^3C^2}f'_G + \frac{4BC'}{rB^3}f''_G - \frac{C'B''}{C^3}f'_G \\
&\quad - \frac{BC'^2}{2C^4}f'_G + \frac{1}{rC^2}f''_G - \frac{B}{2}f + \frac{B'B''}{2rBC^2}f_G \\
&\quad + \frac{3B'^2}{r^2BC^2} - \frac{2C'B''}{rC^3}f_G + \frac{B'^2C'}{rBC^3}f_G \\
&\quad - \frac{5B'C'}{r^2C^3}f_G + \frac{2B''}{r^2C^2}f_G + \frac{5B'}{r^3C^2}f_G \\
&\quad - \frac{B'^4}{4B^3C}f_G - \frac{B'^3}{4B^2C^2f_G} - \frac{BC'^2}{rC^4}f_G \\
&\quad - \frac{B'C'}{4rBC^3}f_G + \frac{B''}{2rBC^2}f_G \\
&\quad - \frac{B'^2}{4rB^2C^2}f_G - \frac{C'}{r^2C^3}f_G \\
&\quad - \frac{BC'}{r^2C^3}f'_G + \frac{4B}{r^3C^2}f'_G + \frac{B}{4C^2}f_G, \qquad (41)
\end{aligned}$$

$$\begin{aligned}
\chi_{11} &= \frac{3B'^2C'}{2B^2C^2}f'_G - \frac{B'C'}{BC^2}f''_G \\
&\quad - \frac{3B'C'^2}{4BC^3}f'_G + \frac{9B'C'}{rBC^2}f'_G - \frac{3B'B''}{B^2C}f'_G \\
&\quad + \frac{B''C'}{2BC^2}f'_G - \frac{6B''}{rBC}f'_G + \frac{5B'^3}{4B^3C}f'_G \\
&\quad - \frac{B'^2}{2B^2C}f''_G - \frac{6B'}{rBC}f''_G - \frac{6B'}{r^2BC}f'_G \\
&\quad - \frac{2C'}{rC^2}f''_G - \frac{C'^2}{rC^3}f'_G + \frac{10C'}{r^2C^2}f'_G \\
&\quad - \frac{6}{r^2C}f''_G - \frac{20}{r^3C}f'_G \\
&\quad - \frac{C'B'^2}{2B^2C^2f'_G} - \frac{B'C'}{2BC^2}f''_G - \frac{B'}{2B^2Cr}f'_G \\
&\quad + \frac{C}{2}f - \frac{B'C'B''}{2B^2C^2}f_G \\
&\quad + \frac{B'^2B''}{2B^3C}f_G + \frac{B'^2C'}{rB^2C^2}f_G - \frac{B'C'}{r^2BC^2}f_G \\
&\quad - \frac{2B''}{Br^2C}f_G + \frac{B'^2}{r^2BC^2}f_G - \frac{4C'}{r^3C^2}f_G \\
&\quad - \frac{B'^2B''}{2B^3C}f_G + \frac{B'C'}{4rB^2C^2}f_G \\
&\quad - \frac{B''}{2rBC^2}f_G + \frac{B'^2}{4rB^3C}f_G - \frac{B'}{r^2B^2C}f_G \\
&\quad - \frac{C'^2}{4C^3}f_G - \frac{C'}{2BC^2r}f_G, \qquad (42)
\end{aligned}$$

$$\begin{aligned}
\chi_{22} &= \frac{B'^2C'r^2}{4B^2C^3}f'_G - \frac{B'C'^2r^2}{BC^4}f'_G + \frac{15B'C'^r}{2BC^3}f'_G \\
&\quad - \frac{B'B''r^2}{B^2C^2}f'_G + \frac{2r^2C'B''}{BC^3}f'_G \\
&\quad + \frac{3B^3r^2}{4B^3C^2}f'_G - \frac{B'^2}{2B^2C^2}\frac{r^2}{2B^2C^2}f''_G \\
&\quad - \frac{3B'^2r}{2B^2C^2}f'_G - \frac{5B'r}{BC^2}f''_G
\end{aligned}$$

$$
\begin{aligned}
&-\frac{19B'}{BC^2}f'_G-\frac{2rC'}{C^3}f''_G-\frac{4C'^2r}{C^4}f'_G\\
&+\frac{4C'}{C^3}f'_G+\frac{24}{rC^2}f'_G-\frac{B'B''r^2}{B^2C^2}f'_G\\
&+\frac{r^2}{2}f+pr^2f_T+\frac{rB'^2C'}{B^2C^3}f_G+\frac{2B'C'}{BC^3}f_G\\
&-\frac{rB'B''}{B^2C^2}f_G-\frac{rC'B'^2}{2B^2C^3}f_G\\
&+\frac{rB'^3}{2B^3C^2}f_G+\frac{B'^2}{B^2C^2}f_G\\
&+\frac{8B'}{rBC^2}f_G-\frac{4C'}{rC^3}f_G+\frac{C'^2}{C^4}f_G, \qquad (43)\\
\delta_0(r) &= r\int\chi_0^0\mathrm{d}r-\frac{2}{r}\int\left(\int\chi_0^0\mathrm{d}r\right)r\mathrm{d}r\\
&-\frac{\rho_0r^2}{3}-\rho_0r\int f_T\mathrm{d}r\\
&-\frac{2\rho_0}{r}\int\left(\int f_T\mathrm{d}r\right)r\mathrm{d}r+\frac{1}{r}\int pr^2f_T\mathrm{d}r.\\
s(r) &= \int rC\chi_1^1\mathrm{d}r-\int rC\chi_0^0\mathrm{d}r\\
&+2\rho_0r\int C\mathrm{d}r-2\rho_0\int\left(\int C\mathrm{d}r\right)\mathrm{d}r\\
&+2\rho_0\int rCf_T\mathrm{d}r, \qquad (44)\\
T^\star(r) &= -\chi^{11'(D)}-\frac{B'}{2C}\chi^{00}-\frac{C'}{2C}\chi^{11}\\
&+\frac{r}{C}\chi^{22}-\frac{C'}{2C}\chi^{11}-\frac{B'}{2B}\chi^{11}\\
&-\frac{2}{r}\chi^{11}-2\left(\frac{P}{C}\right)f'_T-2\left(\frac{P}{C}\right)'f_T\\
&-\frac{\rho B'}{2BC}f_T-\frac{PC'}{C^2}f_T+\frac{2P}{C}f_T-\frac{4P}{rC}f_T\\
&+\frac{f}{\kappa^2-f_T}\left[\frac{-2p}{D}\frac{f'_T}{f_T}-\frac{7}{2D}p'\right],\\
\delta_1(r) &= r\chi_0^0+r\chi_1^1+2prf_T,\\
\delta_2(r) &= r\chi_0^0+r\chi_2^2+2prf_T. \qquad (45)
\end{aligned}
$$

References

[1] P O Mazur and E Mottola, *Proc. Natl Acad. Sci. USA* **101**, 9545 (2004)
[2] C Cattoen, T Faber and M Visser, *Class. Quantum Gravity* **22**, 4189 (2005)
[3] Z Yousaf, K Bamba, M Z Bhatti and U Ghafoor, *Phys. Rev. D* **100**, 024062 (2019)
[4] Z Yousaf, *Phys. Dark Universe* **28**, 100509 (2020)
[5] Z Yousaf, M Z Bhatti and A Rehman, *Chin. J. Phys.* **73**, 493 (2021)
[6] S Ghosh, F Rahaman, B Guha and S Ray, *Phys. Lett. B* **767**, 380 (2017)
[7] Y B Zeldovich, *Mon. Not. R. Astron. Soc.* **160**, 1P (1972)
[8] P Pani, *Phys. Rev. D* **92**, 124030 (2015)
[9] F S N Lobo and R Garattini, *J. High Energy Phys.* **2013**, 65 (2013)
[10] D Horvat and S Ilijić, *Class. Quantum Gravity* **24**, 5637 (2007)
[11] A DeBenedictis *et al*, *Class. Quantum Gravity* **23**, 2303 (2006)
[12] N Bilić, G B Tupper and R D Viollier, *J. Cosmol. Astropart. Phys.* **2006**, 013 (2006)
[13] P Bhar, *Astrophys. Space Sci.* **354**, 457 (2014)
[14] P Martin Moruno, N M Garcia, F S Lobo and M Visser, *J. Cosmol. Astropart. Phys.* **2012**, 034 (2012)
[15] P Rocha, R Chan, M da Silva and A Wang, *J. Cosmol. Astropart. Phys.* **2008**, 010 (2008)
[16] A Banerjee, F Rahaman, S Islam and M Govender, *Eur. Phys. J. C* **76**, 1 (2016)
[17] B Turimov, B Ahmedov and A Abdujabbarov, *Mod. Phys. Lett. A* **24**, 733 (2009)
[18] T Kubo and N Sakai, *Phys. Rev. D* **93**, 084051 (2016)
[19] D Horvat, S Ilijić and A Marunović, *Class. Quantum Gravity* **26**, 025003 (2008)
[20] S Ghosh *et al*, *Ann. Phys.* **411**, 167968 (2019)
[21] Z Yousaf, M Z Bhatti and K Bamba, *Int. J. Geom. Methods Mod. Phys.* **18**, 2150167 (2021)
[22] Z Yousaf, M Z Bhatti and H Asad, *Int. J. Geom. Methods Mod. Phys.* **19**, 2250070 (2022)
[23] Z Yousaf and M Z Bhatti, *Int. J. Mod. Phys. D* **30**, 2150084 (2021)
[24] M Z Bhatti, Z Yousaf and M Yousaf, *Phys. Dark Universe* **28**, 100501 (2020)
[25] M Z Bhatti, Z Yousaf, M Yousaf and K Bamba, *Int. J. Mod. Phys. D* **31**, 2240002 (2022)
[26] M Z Bhatti, Z Yousaf and M Yousaf, *Int. J. Geom. Methods Mod. Phys.* **19**, 2250018 (2022)
[27] S Ray, R Sengupta and H Nimesh, *Int. J. Mod. Phys. D* **29**, 2030004 (2020)
[28] T Harko, Z Kovács and F S Lobo, *Class. Quantum Gravity* **26**, 215006 (2009)
[29] S Ghosh, S Ray, F Rahaman and B Guha, *Ann. Phys.* **394**, 230 (2018)
[30] M Z Bhatti, Z Yousaf and A Rehman, *Phys. Dark Universe* **29**, 100561 (2020)
[31] S W Hawking and G F R Ellis, *The large scale structure of space-time* (Cambridge University Press, 1973)
[32] A Borowiec, W Godłowski and M Szydłowski, *Phys. Rev. D* **74**, 043502 (2006)
[33] S Nojiri and S D Odintsov, *Int. J. Geom. Methods Mod. Phys* **4**, 115 (2007)
[34] D A Easson, *Int. J. Mod. Phys. A* **19**, 5343 (2004)
[35] S Nojiri, S D Odintsov and M Sasaki, *Phys. Rev. D* **71**, 123509 (2005)
[36] I P Neupane and B M Carter, *J. Cosmol. Astropart. Phys.* **2006**, 004 (2006)

[37] M Z Bhatti, Z Yousaf and M Yousaf, *Chin. J. Phys.* **77**, 2617 (2022)
[38] M Z Bhatti, Z Yousaf and M Yousaf, *Int. J. Geom. Methods Mod. Phys.* **19**, 2250120 (2022)
[39] M Sharif and A Ikram, *Eur. Phys. J. C* **76**, 1 (2016)
[40] G Darmois, *Mémorial des Sciences Mathematiques* (Gauthier-Villars, Paris, 1927) Vol. 25
[41] W Israel, *Il Nuovo Cimento D* **44**, 1 (1966)
[42] K Lanczos, *Ann. Phys. (Berlin)* **379**, 518 (1924)
[43] G Perry and R B Mann, *Gen. Relativ. Gravit.* **24**, 305 (1992)
[44] J L Rosa, *Phys. Rev. D* **103**, 104069 (2021)
[45] M Z Bhatti, Z Yousaf and M Yousaf, arXiv:2207.05965 (2022)
[46] F Rahaman, M Kalam and S Chakraborty, *Gen. Relativ. Gravit.* **38**, 1687 (2006)
[47] J M Lattimer and M Prakash, *Phys. Rep.* **621**, 127 (2016)